Deep-level defects at lattice-mismatched interfaces in GaAs-based heterojunctions

2000 J. Phys.: Condens. Matter 12 10153

(http://iopscience.iop.org/0953-8984/12/49/314)

J. Phys.: Condens. Matter **12** (2000) 10153–10160. Printed in the UK PII: S0953-8984(00)17528-9

Deep-level defects at lattice-mismatched interfaces in GaAs-based heterojunctions

T Wosiński, O Yastrubchak, A Mąkosa and T Figielski
Institute of Physics, Polish Academy of Sciences, Aleja Lotnikow 32/46, 02-668 Warsaw, Poland

Received 28 September 2000

Abstract. Electrical properties of lattice-mismatch-induced defects in GaAs/GaAsSb and GaAs/InGaAs heterojunctions have been studied by means of an electron-beam-induced current (EBIC) in a scanning electron microscope and deep-level transient spectroscopy (DLTS). DLTS measurements, carried out with p–n junctions formed at the interfaces, revealed one electron trap and two hole traps induced by the lattice mismatch. The electron trap, at about $E_c - 0.68$ eV, has been attributed to electron states associated with threading dislocations in the ternary compound. By comparing the concentration of this trap, revealed by DLTS, with EBIC results on the diffusion length, obtained for heterojunctions with different lattice mismatches, it is inferred that the minority-carrier lifetime is controlled by dislocations in the epilayer region close to the interface. Two new hole traps have been ascribed to defects associated with the lattice-mismatched interface of the heterostructures.

1. Introduction

Epitaxial growth of lattice-mismatched heterostructures is accompanied by a strain in the epilayer that results from a difference in lattice parameter between the substrate and the epilayer. In semiconductor heterostructures with diamond or zinc-blende structure, epitaxially grown on mismatched (001)-oriented substrates, misfit dislocations lying along two orthogonal ⟨110⟩ directions are generated at the interface to relieve mismatch strain. They are of two general types: pure edge 90° dislocations and mixed 60° dislocations. 90° dislocations relieve the strain more efficiently than 60° dislocations. However, the misfit dislocations are formed only after the growing epilayer reaches a certain 'critical' thickness and the edge dislocations cannot glide to the interface since their glide plane is (001). Therefore, the dominant type of misfit dislocation observed in structures with a small lattice mismatch (less than 2%) are 60° dislocations gliding on {111} planes. 90° dislocations are more often observed in systems with a large lattice mismatch (>2%) where they can be generated easily owing to three-dimensional growth of the epilayer [1]. The misfit dislocations are accompanied by threading dislocations which propagate into the epitaxial layer. Both kinds of dislocation can give rise to energy levels in the band gap which act as recombination centres or traps for free carriers. Eventually, they can lead to a degradation of the performance and reliability of semiconductor devices based on heterostructures.

In GaAs-based heterostructures, 60° misfit dislocations lying along two different orthogonal ⟨110⟩ directions at the interface differ in their core structures. In the predominant glide set configuration, the two dislocation types, referred to as α and β, consist of the extra half-planes terminated by a row of arsenic and gallium atoms, respectively, in the dislocation core.

0953-8984/00/4910153+08$30.00

In the present paper we report results of investigations of electrical properties of lattice-mismatch-induced defects in GaAs-based heterojunctions studied by means of electron-beam-induced current (EBIC) in a scanning electron microscope and deep-level transient spectroscopy (DLTS).

2. Structure growth and CL characterization

We studied two types of heterostructure, GaAs/GaAsSb and GaAs/InGaAs containing a small mole fraction, up to a few per cent, of antimony or indium in the ternary compound. Structures of the first type were p^+–n heterojunctions fabricated by liquid-phase-epitaxy (LPE) growth of $GaAs_{1-x}Sb_x$ layers, on (001)-oriented substrates of p^+-type GaAs doped with Zn. Three structures with different Sb contents in the epilayer ($x = 1$, 2 and 3%) and, in addition, a reference heterostructure without Sb were grown simultaneously to ensure the same growth conditions for the layers. The layers of some tens of μm width were of n type with the free-electron concentration $n \approx 10^{15}$ cm^{-3}. Owing to a diffusion of Zn atoms into the epilayer during its growth at 850 °C, the p^+–n junction position was shifted by a fraction of a μm to the GaAsSb side with respect to that of the heterointerface. Sb content in the epilayers has been estimated by means of spectrally resolved cathodoluminescence (CL) in a scanning electron microscope employed to investigate the angle-lapped heterostructures. The resulting values of $x = 1.1$, 1.9 and 2.7%, obtained from the layer regions of several μm thickness near the interface, were in good accord with the values assumed in the technological process [2].

The second type of structure was an n^+–p heterojunction grown by molecular beam epitaxy (MBE) of an InGaAs layer on a (001)-oriented n^+-type GaAs substrate doped with Si. The 1 μm thick InGaAs layer with the In content of 3% was Si doped to the thickness of 0.3 μm. The upper part of the layer was Be doped to p type at the concentration of 10^{16} cm^{-3}, so the n^+–p junction position was shifted 0.3 μm towards the InGaAs side from the heterointerface.

A difference in lattice constant between the substrate and the ternary compound (about 0.2% at 3% of Sb or In content) resulted in generation of 60° misfit dislocations at the interface to relieve some of the strain in the epitaxial layer. They form a two-dimensional array of α- and β-dislocations lying at the interface along the $[\bar{1}10]$ and [110] directions, respectively. The misfit dislocations have been revealed as dark lines with spatially resolved CL (figure 1) owing to an enhanced rate of non-radiative recombination of electron–hole pairs generated by an electron beam. The larger density of misfit α-dislocations as compared with that of β-ones, visible in figure 1, results from an anisotropy of the glide velocity of the two types of dislocation in GaAs.

3. EBIC results

The GaAs/GaAsSb heterostructures were investigated by means of the EBIC technique using a scanning electron microscope by employing angle-lapped p^+–n junctions formed at the interfaces. The minority-carrier diffusion length was measured using the method proposed by Hackett [3] and the sample configuration shown in figure 2. The method consists in measuring the EBIC current, I, in an angle-lapped p–n junction as a function of the distance, y, of the electron beam from the junction intersection with the lapped surface, which lies at a small angle, θ, with respect to the junction plane. The EBIC current varies exponentially with the distance according to the formula

$$I(y) = I_0 \exp(-y \sin\theta / L) \tag{1}$$

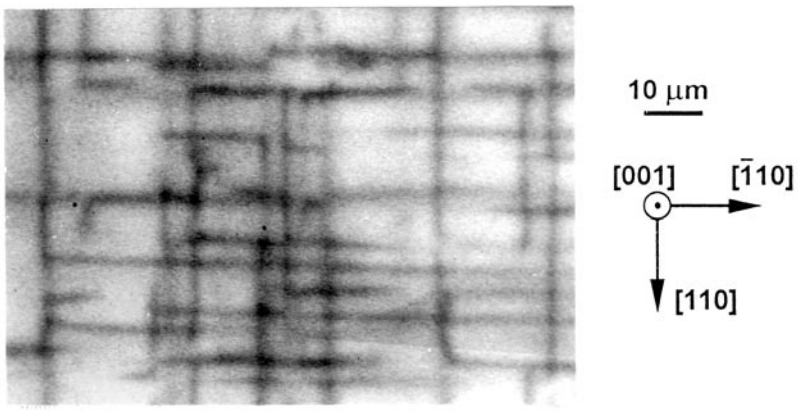

Figure 1. A planar cathodoluminescence micrograph of the interface of a GaAs/$GaAs_{0.97}Sb_{0.03}$ heterostructure revealing misfit α- and β-dislocations as, respectively, horizontal and vertical dark lines.

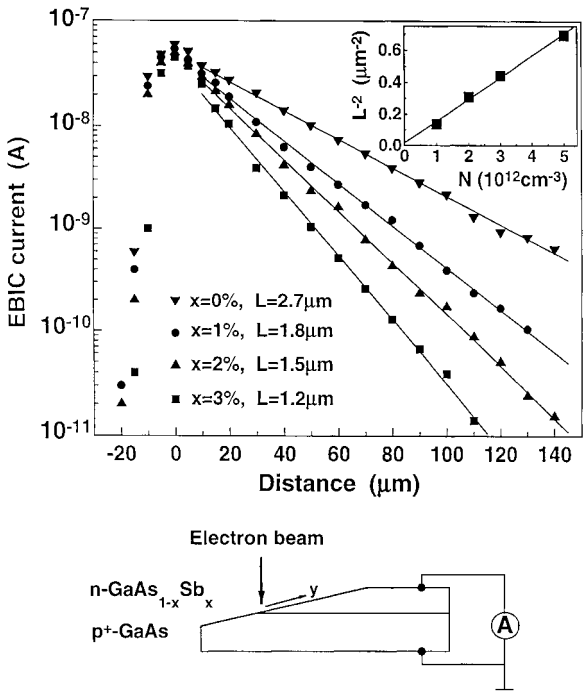

Figure 2. EBIC current versus scan distance along a 5° angle-lapped surface of a GaAs/$GaAs_{1-x}Sb_x$ heterojunction. Lines represent the fitting of equation (1) to the experimental points. The inset shows the inverse square of the hole diffusion length versus the concentration of the ED1 traps in the epilayers with various Sb contents. The sample configuration for the EBIC measurements is shown below.

from which the minority-carrier diffusion length, L, can be determined directly. The current profile (1) is independent of the spatial distribution of minority-carrier excitation and is insensitive to possible variations in the surface recombination velocity [3].

Experimental data for I versus y, measured at an accelerating voltage of 15 kV and a beam current of 3×10^{-11} A, are presented in figure 2. The electron beam was defocused to a rectangle of 10×25 μm^2, with the longer edge parallel to the junction, in order to obtain average values not affected by possible local imperfections. From fitting equation (1) to the experimental data, hole diffusion lengths of 2.7, 1.8, 1.5 and 1.2 μm in the layers with Sb contents of 0, 1, 2 and 3%, respectively, were determined.

The observed decrease in the minority-carrier diffusion length in the epilayers with increasing lattice mismatch suggests that dislocations can be the lifetime-limiting defects in the samples investigated. In our previous paper [4] we discussed reduced minority-carrier lifetime at dislocations in GaAs. Following the model of recombination at dislocations given by Wilshaw *et al* [5], we assumed that the recombination of excess minority carriers (holes) generated by an electron beam can be described by the bulk hole lifetime, τ_b, far away from dislocations and a reduced hole lifetime, τ', within the space-charge cylinders, of radius R, around dislocations. The hole lifetime in the sample containing dislocations, τ, can be related to τ_b and τ' by [4]

$$1/\tau \approx 1/\tau_b + \pi R^2 N_d/\tau' \tag{2}$$

where N_d is the dislocation density in the region investigated and $\pi R^2 N_d$ represents the volume of the space-charge cylinders per unit volume of a crystal. Taking into account that $\tau = L^2/D$, where D is the hole diffusion coefficient, equation (2) predicts a linear dependence of the inverse square of the hole diffusion length on the dislocation density.

4. DLTS results

The spectrum of lattice-mismatch-induced defects has been studied for both types of structure by means of DLTS using p–n junctions formed in the epilayers. This allowed for investigation of both electron traps in the upper half of the band gap and hole traps in the lower half.

4.1. Electron traps

Two electron traps have been revealed in the DLTS spectra in the GaAs/GaAsSb heterostructures, as described in our previous paper [6]. Here, we concern ourselves with the electron trap, called ED1, associated with dislocations. This trap had been, for the first time, revealed, by means of DLTS, in plastically deformed bulk GaAs at $E_c - 0.68$ eV and related to electron states associated with 60° dislocations [7]. The same trap was then found in GaAs/$In_{0.06}Ga_{0.94}As$ heterostructures by Watson *et al* [8] who ascribed the trap to core states of α-dislocations of 60° type on account of the observed correlation between the trap concentration and the density of misfit α-dislocations at the interface.

Extended defects, like dislocations, display a very specific property as electronic traps, which allows us to distinguish them from point defects. It is associated with the Coulomb interaction between a charge carrier just being captured and other charges already captured at the dislocation line. This interaction leads to a characteristic, logarithmic against time, capture kinetics of majority carriers at dislocations [9]. In DLTS measurements it manifests itself as a linear dependence of the signal amplitude on the logarithm of the filling-pulse duration [7]. Such dependence, observed over four orders of magnitude of the filling time for the ED1 trap in one of our GaAs/GaAsSb heterostructures, is shown in the inset in figure 3. In contrast, the amplitude of the EL2 peak, measured simultaneously for the same sample [6], shows a distinct saturation for long filling times. Such behaviour, characteristic of exponential capture kinetics, is typical for isolated point defects.

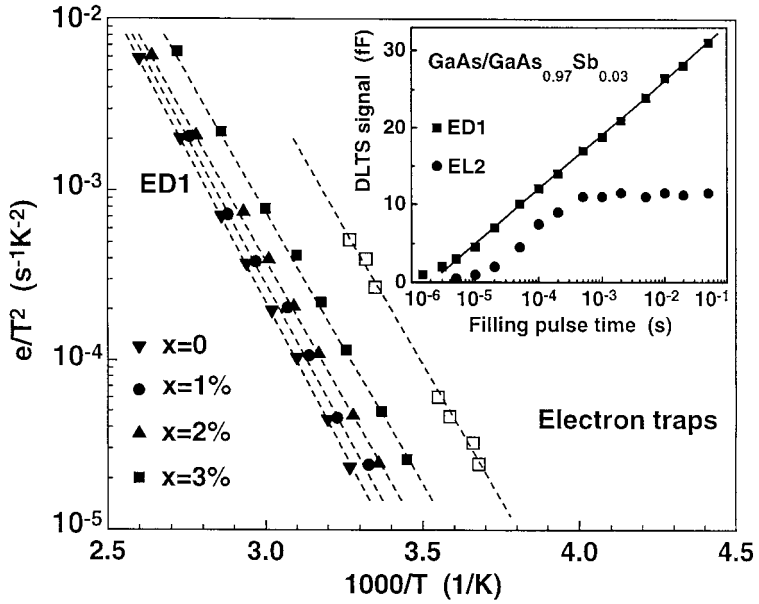

Figure 3. Temperature dependences of the thermal emission rates (Arrhenius plots) for the ED1 electron trap revealed in the GaAs/GaAs$_{1-x}$Sb$_x$ heterostructures (full points) and GaAs/InGaAs heterostructures (open squares). The inset shows DLTS peak amplitudes of ED1 and EL2 traps versus filling-pulse duration measured for the GaAs/GaAs$_{0.97}$Sb$_{0.03}$ heterostructure.

The temperature dependence of the thermal emission rates of electrons from the ED1 trap (Arrhenius plots) measured by DLTS for both GaAs/GaAsSb and GaAs/InGaAs heterostructures is shown in figure 3. We relate the trap to threading dislocations formed in the epitaxial layers of ternary compounds as a result of the lattice mismatch. In the GaAs/GaAsSb heterostructures the concentration of the trap in the region of the epilayer up to about 1 μm from the interface increased with increasing lattice mismatch. It was about 1×10^{12} cm^{-3} in the reference structure and reached a value of about 5×10^{12} cm^{-3} in the epilayer with 3% Sb content. The appearance of the ED1 peak in the DLTS spectrum of the reference heterostructure indicates a large density (about 10^5 cm^{-2}) of dislocations in the GaAs epilayer near the interface. These dislocations originate probably from the p$^+$-GaAs substrate used for the LPE-growth process, which contained a rather large density of grown-in dislocations (etch pit density (EPD) $\approx 5 \times 10^4$ cm^{-2}). In the inset in figure 2 we have plotted the inverse square of the hole diffusion length, measured by means of an EBIC, versus the concentration of the ED1 traps, obtained by DLTS, in the GaAsSb epilayers with various Sb contents. The proportionality between the two quantities is in accordance with the equation (2) and it suggests that, actually, lattice-mismatch-induced dislocations control the minority-carrier diffusion length in the epitaxial layers close to the interfaces. From an extrapolation of the dependence shown in the inset in figure 2 to zero concentration of ED1, one obtains a hole diffusion length of about 7 μm in a crystal without dislocations. In this case, however, other defects would limit the minority-carrier lifetime.

The activation energies of the ED1 trap, evaluated from the slopes of the Arrhenius plots shown in figure 3, decrease with increase of the Sb or In content in the epilayer similarly to how the band-gap energy in the ternary compound decreases. They are presented in figure 4 versus the band-gap energy of the respective compounds. In addition, the result reported by

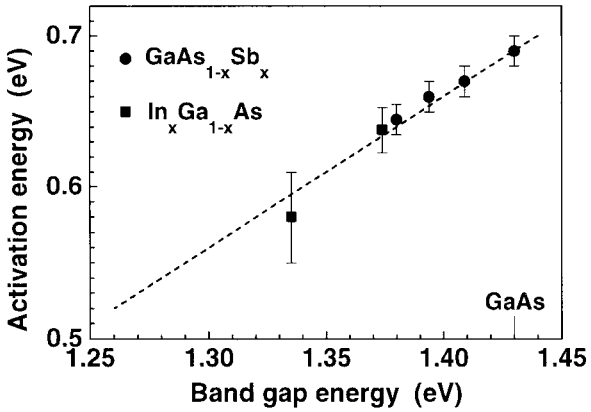

Figure 4. Electron-emission activation energy for ED1 traps versus band-gap energy at 300 K obtained for GaAs/$GaAs_{1-x}Sb_x$ heterostructures (circles) and GaAs/$In_xGa_{1-x}As$ heterostructures (squares). The lowest point, after reference [8], corresponds to $x = 6\%$. The broken line represents the constant position of the trap level with respect to the valence band edge of $E_v + 0.74$ eV.

Watson *et al* [8] for $In_xGa_{1-x}As$ layers with $x = 6\%$ is included in the figure. The observed dependence indicates that the energy level position of the trap with respect to the top of the valence band remains the same in each material, suggesting that the defect state is composed primarily of the valence band states. This strongly valence-band-like character of the ED1 trap is compatible with the identification of the trap with the core states of α-dislocations in which dangling bonds correspond to As atoms [6]. Similar dependence of a trap activation energy on the band-gap energy has recently been found by Pal *et al* [10] for the electron trap attributed to threading dislocations in MBE-grown InGaAs layers with higher (10 to 30%) In mole fraction.

4.2. Hole traps

The evolution of the hole-trap DLTS spectrum as a result of Sb incorporation into the epilayer lattice in GaAs/$GaAs_{1-x}Sb_x$ structures is presented in figure 5. Two hole traps, referred to as A and B, with hole-emission activation energies of 0.40 eV and 0.70 eV and concentrations of 7×10^{13} cm^{-3} and 2×10^{14} cm^{-3}, respectively, have been revealed in the reference structure. These traps, which are commonly observed in LPE-grown GaAs, were assigned to native point defects related to excess gallium in a crystal [11, 12]; however, their precise microscopic nature remains unresolved.

Two new hole traps, called HD2 and HD3 in our previous paper [2], appeared in the DLTS spectra of lattice-mismatched heterostructures. The temperature dependences of the thermal emission rates (Arrhenius plots) for the two traps, together with those for the A and B hole traps, obtained from the heterostructures investigated are presented in figure 6. The hole-emission activation energy of the HD2 trap, 0.51 eV at $x = 1\%$, decreases with increase of the Sb content in the epilayer similarly to the decrease of the energy gap of the $GaAs_{1-x}Sb_x$ compound. Similarly, the activation energies of the traps A and B decrease with increase of the Sb content in the epilayer in such a way that their energy level positions remain constant with respect to the bottom of the conduction band. On the other hand, the activation energy of the HD3 trap, about 0.74 eV, was roughly the same for all of the structures investigated; however, owing to the location of the HD3 peak on the high-temperature slope of the much larger B

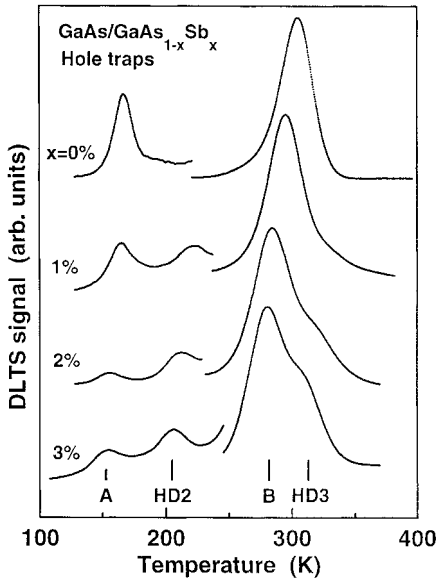

Figure 5. Hole-emission DLTS spectra measured at a rate window of 2 s^{-1} for the GaAs/$GaAs_{1-x}Sb_x$ heterostructures.

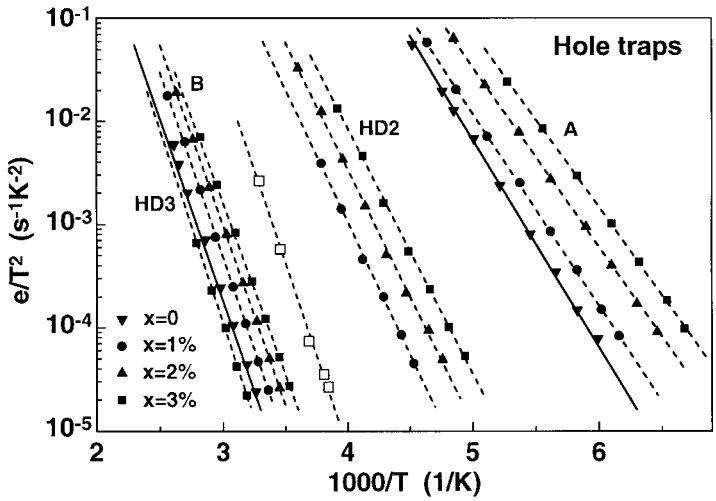

Figure 6. Temperature dependences of the thermal emission rates (Arrhenius plots) for the hole traps revealed in the GaAs/$GaAs_{1-x}Sb_x$ heterostructures (full symbols) and GaAs/InGaAs heterostructures (open squares). Solid lines represent the data for A and B traps in GaAs, after reference [12].

peak in the DLTS spectra, the precise determination of the HD3-trap activation energy was strongly disturbed. The concentrations of the HD2 and HD3 traps increased systematically with increase of the Sb content in the epilayer while the concentrations of the A and B traps decreased. It is worth noting that the hole-trap DLTS spectrum was detected under forward-bias injection when the active DLTS region reached the lattice-mismatched interface.

Only one hole trap, with the activation energy of about 0.71 eV, was found in the DLTS spectrum of the GaAs/InGaAs heterojunction. Its Arrhenius plot is also shown in figure 6. Though its Arrhenius plot is shifted to slightly lower temperatures, we ascribe the trap to HD3

as it was also detected under forward-bias injection. The measurements of the dependence of the DLTS signal intensity of this trap on the filling-pulse duration revealed strongly non-exponential kinetics for capture of holes into the trap states, suggesting its association with extended defects. A detailed analysis of the kinetic behaviour of the trap over a wide range of filling time was, however, not possible owing to the small signal-to-noise ratio, especially for short filling pulses. We tentatively relate the HD2 and HD3 hole traps to defects associated with the lattice-mismatched interfaces in both types of heterostructure—probably to misfit dislocations.

Probably the hole trap recently found by Du *et al* [13] in GaAs/InGaAs lattice-mismatched heterostructures with various In mole fractions and layer thicknesses is the same as HD3. That trap, labelled H4 by the authors, with DLTS activation energy between 0.67 and 0.73 eV, has been related to misfit dislocations at the interface by comparing the DLTS spectra of various heterostructures with the distribution of dislocations revealed by means of transmission electron microscopy.

5. Conclusions

One electron trap and two hole traps, induced by lattice mismatch, have been found with the DLTS technique in GaAs/GaAsSb and GaAs/InGaAs heterojunctions. The electron trap has been attributed to threading dislocations in the layer of ternary compound close to the interface. By comparing the concentration of this trap with the EBIC results for the diffusion length in the same epitaxial layers, it is concluded that the threading dislocations limit the minority-carrier lifetime in the layers. Two hole traps, which have been detected under forward-bias injection when the active DLTS region comprises the interface, are related to defects associated with the lattice-mismatched interface—probably to misfit dislocations lying at the interface in both types of heterojunction.

Acknowledgments

The authors would like to thank J Raczyńska (Warsaw) and B F Usher (Melbourne) for growing the heterostructures investigated, and A Zozime (Bellevue) for cooperation in the CL and EBIC measurements. This work was partly supported by the Committee for Scientific Research of Poland under grant No 2 P03B 063 19.

References

[1] Fitzgerald E A 1991 *Mater. Sci. Rep.* **7** 87
[2] Wosiński T, Mąkosa A and Raczyńska J 1995 *Acta Phys. Pol.* A **87** 369
[3] Hackett W H 1971 *J. Appl. Phys.* **42** 3249
Hackett W H 1972 *J. Appl. Phys.* **43** 1649
[4] Wosiński T, Zozime A, Rivière A and Vermeulin C 1994 *Phys. Status Solidi* a **142** 347
[5] Wilshaw P R, Fell T S and Booker G R 1989 *Point and Extended Defects in Semiconductors* ed G Benedek, A Cavallini and W Schröter (New York: Plenum) p 243
[6] Wosiński T, Mąkosa A, Figielski T and Raczyńska J 1995 *Appl. Phys. Lett.* **67** 1131
[7] Wosiński T 1989 *J. Appl. Phys.* **65** 1566
[8] Watson G P, Ast D G, Anderson T J, Pathangey B and Hayakawa Y 1992 *J. Appl. Phys.* **71** 3399
[9] Figielski T 1978 *Solid State Electron.* **21** 1403
[10] Pal D, Gombia E, Mosca R, Bosacchi A and Franchi S 1998 *J. Appl. Phys.* **84** 2965
[11] Lang D V and Logan R A 1975 *J. Electron. Mater.* **4** 1053
[12] Wang Z-G, Ledebo L-A and Grimmeiss H G 1984 *J. Phys. C: Solid State Phys.* **17** 259
[13] Du A Y, Li M F, Chong T C, Xu S J, Zhang Z and Yu D P 1997 *Thin Solid Films* **311** 7